NOVEL SRF GUN DESIGN*

F. Marhauser#, MuPlus, Inc., Newport News, VA, USA
Z. Li, K. Lee, SLAC, Menlo Park, CA, USA

Abstract

A high brightness superconducting radio frequency (SRF) photoinjector gun cavity has been developed to a level ready for construction. The design aims to prevent operational limitations encountered with existing concepts.

INTRODUCTION

A novel SRF photoinjector gun cavity (short: gun) has been proposed recently for use in next generation small- to large-scale electron facilities such as compact light sources (for industrial and medical uses) and high average power free electron lasers [1]. These facilities demand challenging beam properties from the electron source. Typically, transverse beam emittances in the order of ~1 π mm-mrad (rms) with bunch charges up to 1 nC at repetition rates of 1 MHz and beyond are envisioned. This embraces both high peak and average beam brightness operation. Presently, the combination of these requirements cannot be fulfilled with any DC or RF electron source (normal-conducting or superconducting). Particularly, research for SRF guns has remained an active field since the late 1980s, which implies a rather slow development. Prevalent limitations are mostly related to the photocathode to be inserted into the SRF environment. Due to design complexities and associated vulnerabilities, damage and contamination of the delicate interior and/or photo layer have been encountered repetitively among the differing concepts (i.e. elliptical, quarter wave resonator, DC-SRF hybrid, and Nb/Pb hybrid guns). This prevented from operating stably at the proclaimed field levels either in vertical or horizontal tests (e.g. [2]-[5]). Thus, a blemish-free superconducting surface is the key for success.

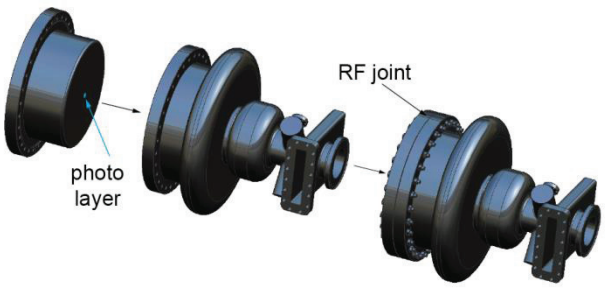

Figure 1: Left to right: Demountable back plate, main gun body, and joined structure. A waveguide input and two HOM couplers attached to the beam tubes are shown.

*Work supported under U.S. DOE Grant Application Number 98802B12-I
e-mail: frank@muplusinc.com

This consideration has led to the concept depicted in Fig. 1. It utilizes a non-conventional accelerating RF mode (TM_{020}) in the first half cell to facilitate a complete exchange of the back wall. Easy access for chemical treatment and high pressure ultrapure water rinsing is granted to aim for high fields at high quality factors, while mitigating field emission, dark currents, and/or multipacting issues. The RF joint between the back wall and the main gun body is facilitated with a flange-gasket connection to allow repetitive access to the interior even after fabrication to eventually rid the cavity from any major contamination. Furthermore, both parts can be fabricated and cleaned independently from each other to be assembled in a clean-room after a final rinse.

A cathode hole in the back wall and a rather complex cathode exchange system is not considered. Associated risks and costs are eliminated. Instead, the back plate carries a photo layer. This concept adopts the idea proposed in the last decade to merely laser-illuminate a photo layer at the center of the back wall (e.g. [6], [7]). A metal cathode - preferably a superconductor - can principally provide unlimited lifetime while being less susceptible to contaminations than delicate mono- or multi-alkali cathodes (e.g. Cs_2Te, CsK_2Sb). Though metal cathodes (incl. Nb) usually exhibit low quantum efficiency (QE), a superconducting Pb photo layer is considered adequate for applications requiring modest average beam currents (~ 1 mA, i.e. 1 nC/1 MHz or 100pC/10 MHz) with reasonable laser power. Specifically, plasma arc-deposition of Pb on Nb has been found to provide the highest QE of up to 0.55 % (in the UV range) among other coating techniques [6]. The successful deposition of a high-quality Pb photo layer (μm-thick) on Nb cavities ('Nb/Pb hybrid guns') has been demonstrated in the past [7]. Yet, the coating process remains delicate. E.g., a Nb/Pb hybrid gun produced recently for HZB/Berlin has suffered a significant Q-degradation after coating when tested in the horizontal cryostat [5]. However, the Pb layer exhibited an uneven profile with droplets that caused elevated field emission. Hence, producing a high quality thin film coating avoiding Pb droplets is mandatory. Practical difficulties during the coating process arise from the fact that the Pb ion beam has to pass the whole cavity. The proposed gun simplifies the coating process since the deposition can be done directly onto the back wall without requiring the main gun body. This offers improved quality control, e.g. immediate optical inspection of the photo layer.

Further details of the gun design are described in the following including RF, thermal and structural aspects.

DESIGN ASPECTS

The main feature granting to remove the back wall is the TM_{020}-mode resonating in the first half cell of the gun. It exhibits a ring with vanishing magnetic fields at a radial offset far away from the cathode. The back wall can be opened at this position with minor RF losses. Subsequent (full) cells can operate in the conventional TM_{010} mode to not significantly compromise the accelerating efficiency. The half cell is larger in diameter to yield the same frequency as a full cell. It can be optimized in conjunction with the aperture radius to, e.g., provide a flat accelerating field along the axis. The principal design is illustrated in Fig. 2 by means of a 1½-cell gun depicting a cutaway view, the surface electric field amplitude, and magnetic flux density from left to right.

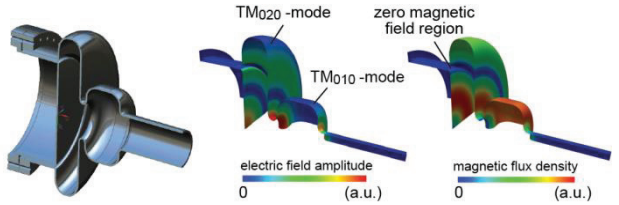

Figure 2: Left to right: Cutaway view and surface electric and magnetic field contours.

The demountable back wall is joined to the gun body via a flange-gasket connection. This inevitably creates a coaxial line. Though the magnetic field vanishes at the beginning of the line, the electrical field exhibits a local maximum. Residual RF fields then still leak into the line towards the end of the filter. The rejection of the fundamental mode can be done efficiently by choosing the appropriate length of the line (close to λ/2). Note that the following absolute results refer to a 1.5 GHz design, though the geometry is scalable to any frequency. The practical objective is to sustain a surface field as high as 50 MV/m at the cathode layer, which is essential to limit space charge forces at the origin. Normalized to this value, Fig. 3 plots the electrical field (black) and magnetic flux density (red) along the surface interior from the cathode to the beam tube end. The extent of the back wall, filter line, 1st cell, iris, and 2nd cell are marked on the left.

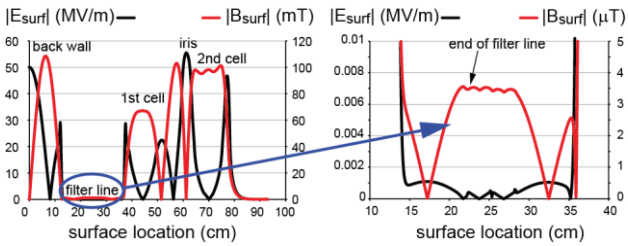

Figure 3: Absolute surface RF electric (black) and magnetic flux density (red), respectively, along the surface interior.

The right figure is a magnified view of the surface fields within the filter line. The simulation includes the features of a flat gasket pressed between two flanges. It reveals that the magnetic flux density is in the μT-regime all along the RF joint. This is a flux density comparable to that far within the beam tube, i.e. where cavities are routinely connected with each other not requiring a superconducting joint. Moreover, a few μT inhibit thermal runaways of the cavity even in case the flanges and the gasket are in a normal conducting state. A corresponding thermal calculation using stainless steel flanges (SS 316L) and a copper (OFHC, RRR = 100) gasket is shown in Fig. 4 (five degree slice model).

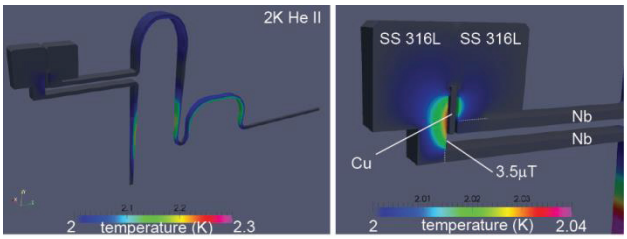

Figure 4: Thermal distribution in the SRF gun walls operating in CW mode (50 MV/m at cathode).

The simulations were conducted with the supercomputing code TEM3P that allows for the non-linear properties of all materials and the Kaptiza resistance at the metal/He interfaces [8]. Note that the details of a standard ConFlat flange with knife edges and a crushed gasket have been modelled. The materials used are indicated in the right plot, which is a closer view around the RF joint. The gun is fully immersed in superfluid helium (He II) at 2 K. The result reveals that the temperatures at the normal conducting RF joint reach only 2.04 K in maximum.

Further calculations have been performed to study the effect of laser heating at the photo layer (Ø = 3 mm). The laser deposits additional power (P_{laser}) depending on the QE of the cathode at a given average beam current (I_{ave}). The absorbed power is $P_{laser}\cdot(1\text{-}R\text{-}QE)$ with R denoting the reflectivity of the photocathode. To be most conservative, R and QE were set to zero such that the full laser power was applied as a heat source. A calculation with $P_{laser} = 2.6$ W to obtain $I_{ave} = 1$ mA (QE = 0.27 %, half of max. for Pb) resulted in a peak temperature of 2.72 K in the mid of the cathode layer. Hereby, the higher temperatures around the cathode are confined to a fraction of the Nb wall thickness, thus not causing a thermal runaway. In a separate calculation a normal conducting layer (Cu) has been assumed instead of Pb. Even in this case the temperatures were confined similarly around the cathode (max. 2.62 K) since the RF magnetic flux density vanishes at the center. The finding implies that the use of a normal conducting photo layer is a feasible option.

Note that up to the dome region, flat walls have been employed for the half cell to not only ease fabrication, but to symmetrize the fields between adjacent walls. This makes the filter efficiency less susceptible to fabrication tolerances. For instance, a major contributor to geometrical inaccuracies is the known springback effect of the cavity sheet material after deep-drawing. It

typically results in up to 100 µm deviations from the ideal profile. For the flat walls the springback effect is mostly eliminated or can be reversed, but still can affect the dome region. Tolerance studies have been performed that considered deviations from the ideal geometry. For instance, a geometrical change of the filter line length from its optimum by as much as ± 2 mm caused a negligible increase of field levels (merely 0.1 µT). Most critical is a radial mismatch of the filter's center line with respect to the zero magnetic field. A filter mismatch of ± 0.5 mm from its ideal location (i.e. ~5× the max. expected springback effect) resulted in an elevation of the peak flux density to maximally 1.2 mT at the RF joint. This value is still far below critical field levels of possible superconducting flange (e.g. NbTi, NbZr, NbN) and gasket (e.g. Nb, In, Pb) materials, but becomes critical if one relies on normal conducting materials only (1e5-1e6 higher resistances). Thermal calculations in case of such a mismatch (+ 0.5mm) have been performed for different combinations of flange (SS 316L, NbTi) and gasket (Cu, AlMg, Nb) materials. The results are documented in Fig. 5. While a pure normal conducting connection (SS 316L + Cu) would lead to a thermal runaway (case 1), all other cases are feasible. The crucial result is that conventional NbTi flanges can be used in combination with normal conducting gaskets (Cu or AlMg).

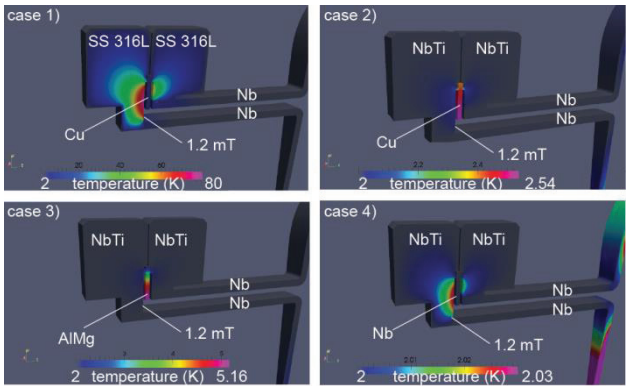

Figure 5: Thermal distributions as in case of Fig. 4, but with a filter line misplaced by +0.5mm from its ideal position. Four cases with material combinations have been studied as indicated.

The gun design also addressed the suppression of multipacting (MP) in the cavity cells and the filter line. Geometrical cell optimizations (for the dome region) have led to soft MP barriers (if at all), e.g. with secondary impact energies below those in standard TESLA cavity cells. This is seen in Fig. 6 (left) indicating the improvement from an initial (gray) to the final design (green) covering operating regimes up to 100 MV/m at the cathode. Analytical calculations have been performed for the filter line concerning potential two-point MP between the walls (Fig. 6 right). The filter gap width has been varied within 1-10 mm and possible resonant MP conditions up to the 5th order (n) studied. The blue area indicates the electric amplitudes feasible for a gap width of 6 mm at 50 MV/m at the cathode. These fields are 1-3 orders of magnitude lower than required for any MP resonance to take place, which also provides a margin concerning geometrical tolerances. The absence of MP in the filter line was confirmed by numerical studies.

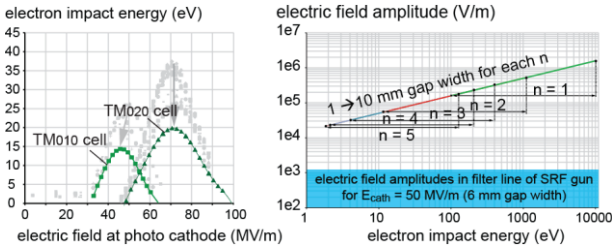

Figure 6: Multipacting assessment for the cavity cells (left) and the filter line (right). See text for more details.

Eventually, structural analyses were carried out to assess the static Lorentz force detuning under different mechanical constraints that allowed obtaining -0.6 Hz/(MV/m)^2 in best case. Beam dynamical studies for a split photoinjector setup with a short linac demonstrated the high brightness performance (see also [1]) and revealed that a 2½ -cell gun is most favourable. Furthermore, the generator power requirements have been assessed in presence of microphonics (less than 10 kW), while different coupler designs were conceived (coaxial, waveguide). One additional benefit is that the TM_{020}-mode grants attaching HOM waveguide couplers directly on the cell (opposite to filter) without creating a surface field enhancement. Further work included the engineering design reusing CEBAF cavity coupler hardware to minimize effort and project costs and commence with the fabrication at our envisioned partner institution JLab.

DISCUSSION

A novel SRF gun has been developed up to an engineering design ready for construction. The ultimate goal was to build and high power test a prototype to demonstrate stable operation at higher than presently achievable field levels in presence of a photocathode layer. The work has been funded as part of the Small Business Innovation Research program (Phase I) by the US Department of Energy (DOE) for a one year period. Funding beyond phase I however was not granted by the DOE, such that any further activities have been halted.

ACKNOWLEDGEMENT

The authors like to thank James Henry at JLab for his support related to the computer-aided engineering design.

REFERENCES

[1] F. Marhauser et al., Proc. IPAC 2012, New Orleans, USA.
[2] A. Arnold, J. Teichert, PRST-AB 14, 024801 (2011).
[3] P. Kneisel, TTC Meeting, JLab, 5-8. Nov. 2012, USA.
[4] W. Xu et al., Proc. PAC 2011, New York, USA.
[5] J. Knobloch, TTC Meeting, JLab, 5-8. Nov. 2012, USA.
[6] J. Smedley et al., PRST-AB 11, 013502 (2008).
[7] J. Sekutowicz et al., Proc. PAC 2009, Vancouver, Canada.
[8] K. Ko et al., Proc. Linac 2010, Tsukuba, Japan.